CPP

Contributions to Plasma Physics

www.cpp-journal.org

WILEY-VCH

REPRINT

Contrib. Plasma Phys. **53**, No. 1, 86 – 91 (2013) / **DOI** 10.1002/ctpp.201310015

On the Use of a Retarding Field Energy Analyzer for Plasma Flow Analysis

Å. Fredriksen[1]*, **W. J. Miloch**[1,2], **N. Gulbrandsen**[1], and **L. N. Mishra**[1,3]

[1] Department of Physics and Technology, University of Tromsø, 9037 Tromsø, Norway
[2] Department of Physics, University of Oslo, Oslo, Norway
[3] Department of Physics, Tribhuvan University, Lalitpur, Neapel

Received 15 December 2011, accepted 07 March 2012
Published online 09 January 2013

Key words Plasma flow, probe diagnostics, retarding field energy analyzer, PC simulations.

Measurements of plasma flow are of key interest in a number of plasma environments and applications. In laboratory magnetized plasmas, the directional Langmuir or Mach probe is a well-proven 'in-situ' diagnostic tool to obtain the flow velocity. However, in non-magnetized or weakly magnetized plasmas, this method does not readily yield reliable velocity measurements, as it has been shown by numerical and experimental studies that the collection of upstream ions to the rearward probe surface can be significant. In this study, we have utilized the analysis of data from 3D PIC simulations [W. J. Miloch, Plasma Phys. Contr. Fusion **52**, 124004 (2010)] of ion velocity distributions in the vicinity of a negatively biased object embedded in a collision-less, source-free plasma with and without flow. The simulations allow us to study how the grounded probe housing of a retarding field ion energy analyzer (RFEA) affects the distribution of ions and their collection at different angles with flowing, electropositive plasma. We find that an analysis based on derived plasma potential at different angles with the flow, may provide more consistent results than the Mach probe theory in our weakly magnetized case. Comparisons are carried out with RFEA measurements in an inductively coupled helicon plasma.

1 Introduction

Plasmas flow with respect to an inertial system is an important parameter in many plasmas, whether it is a plasma rocket exhaust nozzle, a geographical position, or with respect to a probe or an obstacle in a laboratory device. Flows may provide important information about their driving forces and the dynamics of the particular plasma system, e.g. ExB-drifts, plasma thrust, or plasma expansion. The flow of plasma along expanding magnetic field lines occurs in many natural plasmas, like for instance plasma outflow from the solar corona [1, 2], or ion outflow from the polar ionosphere[3, 4].

Furthermore, it is long established that flows in plasmas help lowering the threshold of instabilities [5], and more recently, it has been shown that cross-field turbulent transport in tokamaks can generate parallel flows [6] and play a role in plasma confinement. The study of plasmas and instabilities with flows and ion beams is one of the main objectives behind the construction of the Njord device [7, 8], in which the flow measurements in this article are performed.

In this paper, we investigate the use of a RFEA to diagnose flow along expanding magnetic field lines in the weakly magnetized, steady-state plasma of the Njord helicon device. The RFEA can be turned around its through-feed axis perpendicular to the flow, so that the RFEA aperture can be pointed at arbitrary angles with respect to the flow. The diagnostics problem may be approached with two different methods. The first method is by means of the well-known Mach-probe analysis [9] in which the ratio between ion-saturation currents to a probe surface in the parallel and anti-parallel direction defines the Mach number, i.e. the flow speed in terms of ion sound speed c_s. This method is well proven and widely adopted in magnetized plasmas [10]; while in non-magnetized plasmas it is more disputed [11]. The other method is a straightforward measurement of the plasma potential,

* Corresponding author. E-mail: ashild.fredriksen@uit.no

taking the difference of the potential measured in the anti-parallel direction and in either the perpendicular or parallel direction to flow. Measuring potential differences as a means of directed energy diagnostics is well known from e.g. the characterization of beam energy with respect to a background plasma potential [12], but has to our knowledge not been much reported in connection to flow measurements.

In Section 2 we describe the experiment, simulations, and diagnostics used to study the beam and flow formation and how it is affected by the shaping of the downstream magnetic field. The analysis of flow in data from simulations and experiments is discussed in Section 3.

2 Experiment and simulations

The Njord device consists of a 0.6 m diameter and 1.5 m long chamber with a spherical dome at one end. A helicon plasma source is attached to a 200 mm port at the top of the dome, as shown in Fig. 1. The source is constructed from a 30 cm long Pyrex glass tube with an inner diameter of 13.8 cm. The outer edge of the tube is chosen as origo of the z-axis for measurements along the centre of the column. A Boswell-type saddle antenna is formed around the circumference of the tube. The tube and antenna are enclosed by a cylindrical aluminium former holding a pair of magnetic field coils with a diameter of 24 cm and 9.5 cm width. The centre of the first coil is placed 18 mm downstream of the outer edge of the Pyrex tube, and the centre of the second coil is displaced by 20 cm with respect to the centre of the first. A current of 6 A in both coils produces maxima of the magnetic fields of about 25 mTesla. A 68 cm diameter, 3^{rd} coil (guide coil) is placed 58 cm downstream from origo, close to the intersection between the dome and the main chamber. It produces about 8 mTesla at 20 A current. Large amplitude 13.56 MHz RF power, typically 300 – 800 W forward and less than 50 W reflected, is fed from a Henry 8K Ultra amplifier to the antenna through an air-cooled π-matching network consisting of two variable vacuum capacitors. Three radially and one axially oriented 40 mm ports of the dome are placed 50 cm downstream from origo. Probes can be inserted through these ports, providing measurements along the axial and radial directions.

For the data presented here, a retarding field energy analyzer (RFEA) was used to obtain plasma density and potential, as well as beam density and –energy. The RFEA placed in the radial port (Fig. 1a) could be rotated 360^o around its own axis. The grids and plates of the RFEA were organized 0.7 mm apart as follows; a grounded aperture plate with a gridded opening 2 mm in diameter, an electron repeller grid biased at typically -90 V, a discriminator grid swept from -100 to +100 V at zero offset, a secondary electron repeller grid biased at -18 V, and a collector plate at -9 V with respect to ground. To capture the energy distribution at the plasma potential, additional batteries between the sweep and the grid produced positive offsets up to 90 V in steps of 9 V. The discriminator was biased in 400 steps per sweep. At each step, the collector current, measured over a 37 kΩ resistor, was digitized into 300 samples which were then averaged into one single value, and written to file together with the bias voltage for further processing.

In the experiments reported here, the following parameter settings were used: RF power 400-600 W and Argon gas fill pressure from 0.013 to 0.02 Pa (1.2 – 1.5 sccm). The current in the first and second source coils were set to 5 and 7 A, respectively, where the first is at the outer end of the source. The current in the 3^{rd} coil was varied between 0 and 30 A. Some resulting B-fields are shown in Fig. 1b).

To simulate the plasma flow around a grounded object analogue to the analyzer, particle-in-cell (PIC) numerical simulations were carried out. We employed the DIP3D code, which was designed for simulations of objects in complex plasma environments [13, 14]. For the present study, the code was upgraded to account also for an external uniform magnetic field [15] and collisions [16].We simulated an argon plasma with parameters close to the conditions in the helicon plasma of Njord, except for the plasma density of n=10^{14} m^{-3}, which is two orders of size lower than in Njord, but as high as was allowed for in the simulations, with regards to the computer time available to perform the simulations. The neutral gas density n_n= 2x10^{19} m^{-3}, similar to the experiment. The electron and ion temperatures are T_e = 4 eV and T_i = 0.4 eV, respectively, resulting in a Debye length λ_D = 0.6 mm. The plasma is weakly magnetized with B = 0.1 T, which is set a factor 10 higher than in the experiment in order to keep the same ratios between the Debye length, Larmor radius and probe size as in the experiment. For these plasma parameters, we consider plasma that is flowing with a subsonic velocity along the x-axis (z-axis in the experiment). A spherical analyzer of diameter d = 1.1 cm is placed in the centre of the simulation box of length L=10 cm in each direction. The orifice of radius a/d = 0.1. The acceptance (opening) angle, given by the

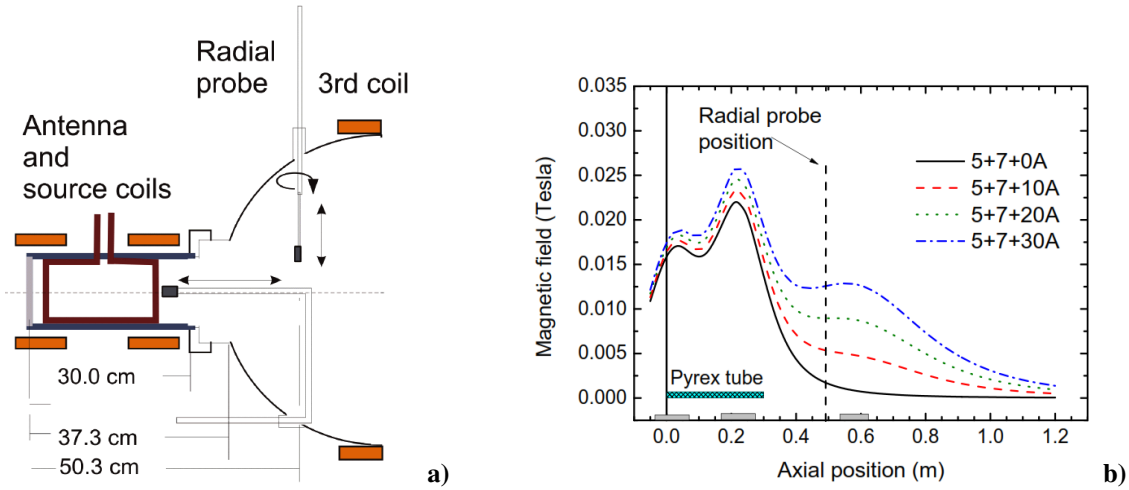

Fig. 1 RF source with probe positioning **a)**, and axial magnetic field **b)** for four different currents in the 3rd coil. Positions of the source glass tube and the coils are indicated at the x-axis.

radius of the aperture and the distance between the aperture and the collector in the experiment, was varied and directed either upstream (anti-parallel) or downstream (parallel) with respect to the flow [17-19]. The surface of the analyzer is set to ϕ = -45 V with respect to the plasma potential, in order to simulate the experimental condition of a grounded analyzer in an electropositive plasma.

3 Results and discussion

To obtain the ion distribution function (IDF), the current vs. bias trace (IV-curve) from the RFEA collector was differentiated with respect to voltage. Figures 2a) and b) show typical IDFs obtained with the aperture of the RFEA face pointing in the anti-parallel (facing the source) and parallel (downstream) directions, respectively, in a case with an ion beam originating from a double layer in an upstream position with respect to the probe. The beam is seen as a second peak in the distribution when the probe is facing the source, as in Figure 2a). The Gaussian fit to the double peaked derivative is also shown. The position of the tallest peak denotes the plasma potential, the difference between the peak maxima provides the beam energy, and the areas of the two Gaussians provide a measure of the respective ion current contributions.

Note that when the probe is facing the downstream direction from the source, no beam is seen, but the distribution is slightly skewed towards lower energies. Furthermore, it should be noted that the acceptance angle of the probe is about 80°.

In the simulations, the same qualitative features as in the probe data are seen. From scrutinizing the simulated data with the probe pointing downstream, the skewness towards lower energies can be explained as originating from particles entering the probe aperture at other angles than normal to the surface. In the simulations, it was also observed that the number of particles with low energy (in the direction towards the probe) contributing to the probe current, increased significantly with acceptance angle of the probe [17]. On the other hand, the simulations showed that the IDFs looking in the upstream direction did not change with acceptance angle. One consequence of this particular property is that the ratio between upstream and downstream currents to the probe is very sensitive to the acceptance angle, as shown in Figure 3. As it is well known, the Mach analysis is only applicable to Maxwellian ion distributions without beam, and hence, these simulations were performed without beam. In Figure 3, current ratios from simulations of plasma flows with Mach numbers 0.4, 0.6, and 0.8 of the ion sound speed c_s as a function of acceptance (opening) angle are shown. Expected current ratios can be found from Mach-analysis, as [20]

$$\frac{I^+_{sat}(\theta)}{I^+_{sat}(\theta+\pi)} = \exp\left(KM\cos\theta\frac{\sin\Delta\theta}{\Delta\theta}\right)$$

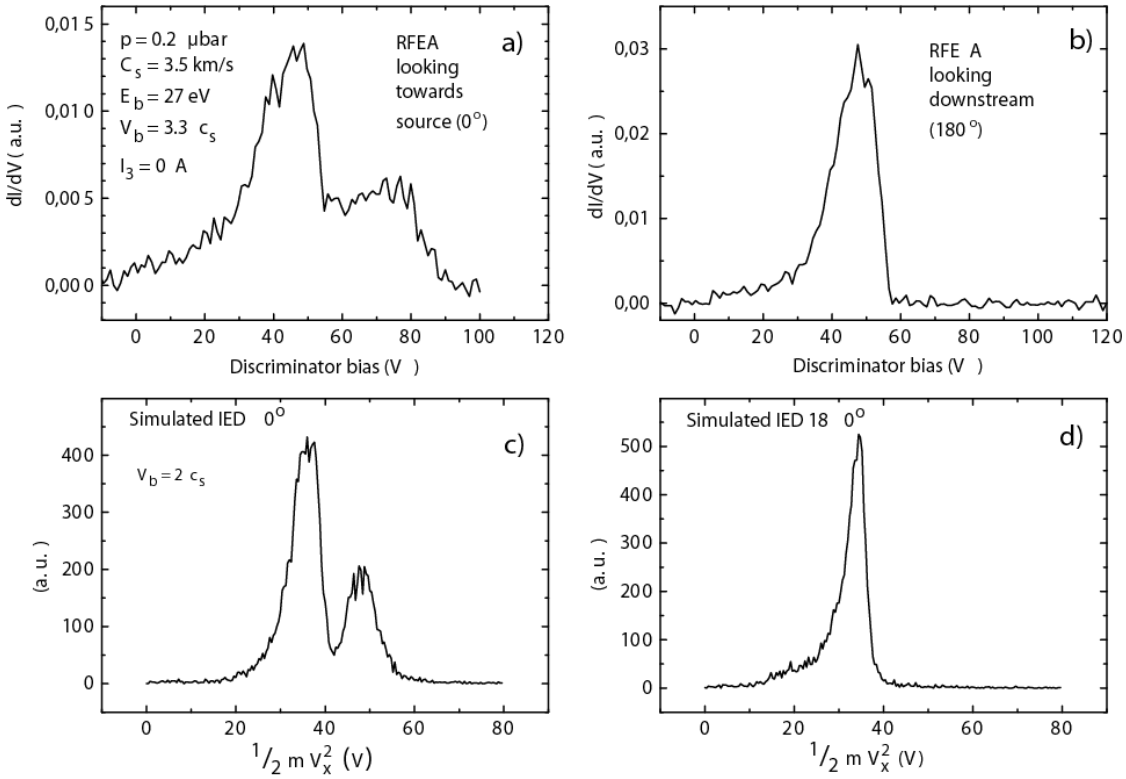

Fig. 2 Ion distribution functions (IDFs) obtained from the RFEA probe facing the plasma source, i.e. upstream direction **a)** and facing the downstream direction **b)**. Ion distribution functions from PIC simulations are shown for a similar case, with a beam speed of 2 c_s, with the probe aperture in the upstream direction **c)** and in the downstream direction **d)**.

As $\theta = 0$ is denoting the upstream direction, the expression can be simplified to

$$\frac{I^+_{sat}(0)}{I^+_{sat}(\pi)} = \exp\left(KM\frac{\sin\Delta\theta}{\Delta\theta}\right) .$$

Here, $\Delta\theta$ is the field of view, or the acceptance angle, of the probe. The constant K depends on magnetization, and in this case we use K = 1.5, as given for a weakly magnetized case, although a value of K = 1.26 for T_i/T_e = 0.1 might be more appropriate [21]. The expected ratios are shown as lines in the plot. It is readily seen that the range of acceptance angles which yield current ratios in agreement with those expected from the given Mach numbers, is very narrow, i.e. somewhere between 30 and 45 degrees. This imposes a quite strict condition on the probe design and construction.

The areas under the IDFs, representing the ion saturation current to the RFEA, were obtained by fitting Gaussian distributions to the IDFs. These were obtained for the RFEA pointing upstream (0°), downstream (180°), and at 90° with respect to the plasma flow into the main chamber. The procedure was carried out for a range of magnetic field currents from 0 A to 35 A in the 3rd coil, resulting in fields from 2 – 15 mTesla at the probe. The IDF areas as a function of 3^{rd} coil current are shown in Figure 4a). At low magnetic fields, a beam from a double layer upstream from the probe could be derived from the IDF of the probe pointing upstream. In this case, the IDF is not Maxwellian, and hence, the Mach probe analysis is not applicable. On the other hand, at a coil current of about 10 A the beam disappears and a single Gaussian can be fitted to the IDFs. This transition has been discussed in more detail in [8]. In Figure 4b), the ratios 0°/180° and 0°/90◦ of total ion currents are shown, exhibiting a ratio of about 2.5 at the coil current where the Mach probe theory becomes applicable. From Equation 1, this ratio indicates a flow speed close to one Mach, with the acceptance angle of the probe being

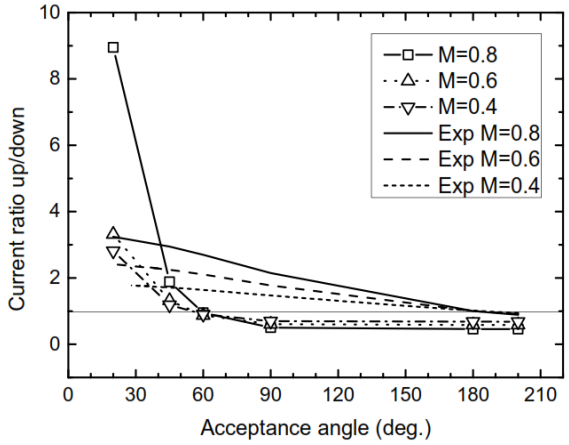

Fig. 3 Current ratios derived from the analysis of simulated data at three different flow speeds given in Mach numbers (lines with symbols). Ratios expected from the Mach probe theory (exp M) with the same speeds are shown for comparison.

about 80°. However, as the simulated data results in much lower values with this acceptance angle, it is likely that the current ratios from the RFEA also underestimate the actual flow values.

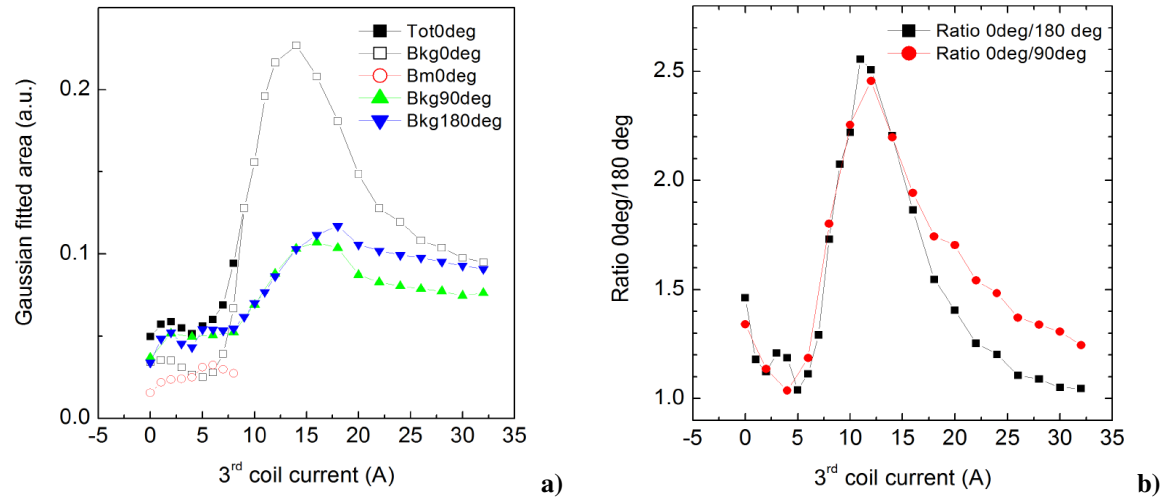

Fig. 4 **a)** Plasma background ion current areas from Gaussians fitted to measured IDFs as function of 3^{rd}coil current in the centre of the plasma column at z=51 cm, with RFEA pointing towards the source at $\theta = 0°$ (open squares), and at $\theta = 90°$ and $\theta = 180°$ away from the source (upward and downward pointing triangles, respectively). Beam areas are shown as open circles, and filled squares denotes the sum of beam and background areas. **b)** Ratios between ion currents at $\theta = 0°$ and $\theta = 180°$ (squares) and between $\theta = 0°$ and $\theta = 90°$ (circles).

Potential difference between the plasma potentials of the probe pointing towards and at $\theta = 180°$ or $\theta = 90°$ away from the source, provides another means of flow analysis. The potential difference can be directly converted to speed as $2\nu_i = \sqrt{2e\Delta V/m_i}$, assuming the difference is taken between upstream and downstream directions. A test of the same set of simulated data as above, with respect to this analysis is shown in Figure 5a).

Velocities obtained from potential differences looking in the $\theta = 0°$ and $\theta = 180°$ directions of the undisturbed ion velocity distribution in the plasma provides a check that the potential difference method is providing the expected results, which it does at Mach numbers > 0.5. Likewise, the differences between the IVDs sampled at the probe in the $\theta = 0°$ and $\theta = 90°$ directions yield velocities close to the expected values, with a small overestimation. The difference between the $\theta = 0°$ and $\theta = 180°$ directions for which the speed is calculated, however, results in velocities overestimated by up to 50% for the lowest Mach numbers. Applying the analysis on the experimental data (Figure 5b), we obtain slightly higher flow velocities from the difference between $\theta = 0°$ and $\theta = 180°$, than between $\theta = 0°$ and $\theta = 90°$ directions, as was predicted from the simulations. The velocities resulting from this analysis are also significantly larger, about 1.2 Mach or about 1.2 times the maximum flow

speed obtained from the density ratios of the same data. This is in agreement with the findings that the simulations indicate that speed is underestimated with Mach analysis. The potential difference method provides a more consistent result in that the flow persists also at higher magnetic field. For the B-field where the beam vanish, the flow speed of the background plasma increases from subsonic to slightly supersonic.

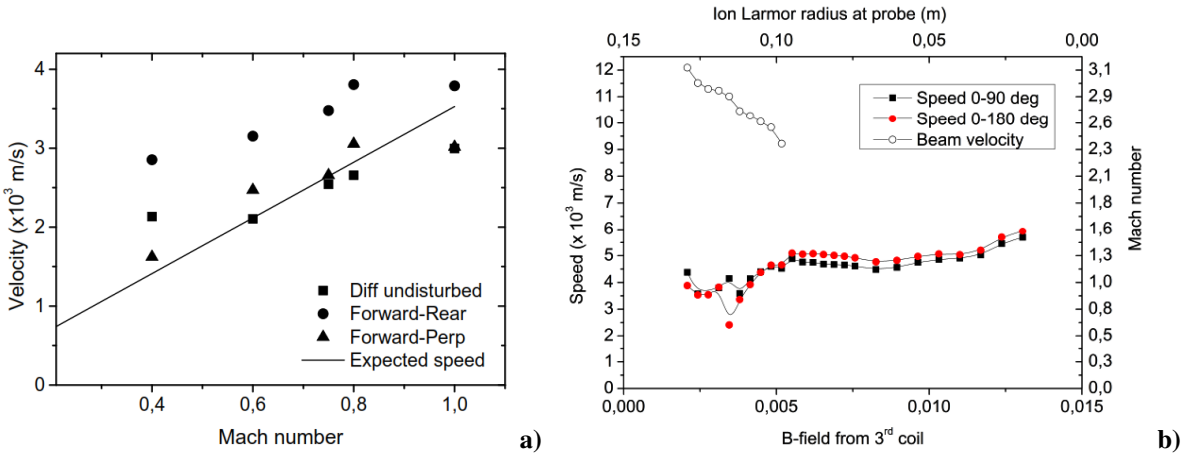

Fig. 5 **a)** Velocities obtained from potential differences in simulated data, as a function of Mach number, between upstream and downstream potentials of undisturbed ion distribution (squares), upstream and downstream collected IVD (circles), and upstream and normally collected IVD (triangles). Expected ion velocities (lines) are plotted for reference. **b)** Beam velocities (open circles), and background plasma velocities (filled squares and circles) from experiment, probe at z=51 cm plotted as a function of B-field from 3^{rd} coil current, the latter obtained from the potential differences between RFEA pointing towards the source and at 90° (filled squares), and at 180° (filled circles) away from the source.

Acknowledgements Part of this work was funded by Norwegian Research Council, Grant no 177570. The authors are grateful to I. Strømmesen, T. Roaldsen, and Y. Eilertsen for their expertise technical assistance, which was essential for operation of this experiment.

References

[1] E.N. Parker, Astrophys. J. **133**, 1014 (1961).
[2] R. Esser, R.J. Edgar, and N.S. Brickhouse, Astrophys. J. **498**, 448 (1998).
[3] U.P. Lovhaug, T. Hagfors, and A.P. van Eyken, Radio Sci. **36**, 1509 (2001).
[4] M. Oieroset et al., J. Geophys. Res. A **104**, 24915 (1999).
[5] Z.Y. Pu et al., J. Geophys. Res. A **104**, 10235 (1999).
[6] C. Hidalgo et al, Phys. Rev. Lett. **91**, 065001 (2003).
[7] H.S. Byhring et al., Phys. Plasmas **15**, 102113 (2008).
[8] A. Fredriksen, L. N. Mishra, and H. S. Byhring, Plasma Sources Sci. & Technol. **19**, 034009 (2010).
[9] M. Hudis and L. M. Lidsky, J. Appl. Phys. **41**, 5011 (1970).
[10] C. Riccardi, R. Barni, and A. Fredriksen, Rev. Sci. Instrum. **75**, 4341 (2004).
[11] I.H. Hutchinson, Phys. Plasmas **9**, 1832 (2002).
[12] C. Charles and R. Boswell, Appl. Phys. Lett. **82**, 1356 (2003).
[13] W.J. Miloch, Plasma Phys. Contr. Fusion **52**, 124004 (2010).
[14] W.J. Miloch, M. Kroll, and D. Block, Phys. Plasmas **17**, 103703 (2010).
[15] C.K. Birdsall and A.B. Langdon, Plasma Physics via Computer Simulation. 1991, Bristol: Adam Hilger.
[16] V. Vahedi and M. Surendra, Comp. Phys. Comm. **87**, 179 (1995).
[17] W.J. Miloch et al., Appl. Phys. Lett. **97**, 261501 (2010).
[18] W.J. Miloch et al, Phys. Plasmas **18**, 083502 (2011).
[19] A. Fredriksen et al, J. Phys. Conf. Ser. **257**, 012019 (2010).
[20] T. Shikama et al., Phys. Plasmas **12**, 044504 (2005).
[21] K.S. Chung et al, Phys. Fluids B **1**, 2229 (1989).